INSTITUTE OF PLASMA PHYSICS
OF THE CZECH ACADEMY OF SCIENCES

BOUNDARY CONDITIONS IN THE GBS SIMULATION OF THE COMPASS TOKAMAK

P. MACHA[1,2],

SUPPORTED BY: D. GALASSI[3], D. OLIVEIRA[3], J. SEIDL[2], D. TSKHAKAYA[2]

List of affiliations:

1) Institute of the plasma physics of the CAS
2) Faculty of nuclear science and physical engineering
3) Ecole Polytechnique Fédérale de Lausanne (EPFL), Swiss Plasma Center (SPC)

EUROfusion

GAČR CZECH SCIENCE FOUNDATION

Tento projekt je spolufinancován se státní podporou Technologické agentury ČR v rámci Programu THÉTA.
www.tacr.cz
Výzkum užitečný pro společnost.

OUTLINE

- Boundary condition types
- BCs used in COMPASS simulation and simulation domain
- An impact of BCs on turbulence
- Impact of BCs on electron velocities and vertical electric field
- Conclusion

GLOBAL BRAGINSKII SOLVER

- First principle, 3D, flux-driven, global, turbulence code for plasma edge simulations based on Braginskii equations [1].
- Full plasma volume, Divertor geometry, electromagnetic effects, kinetic neutrals, ion temperature dynamics, self-consistent turbulence evolution.
- High computational requirements (~2000 cores, ~5-10 M CPU hours).
- Validation on COMPASS tokamak – first validation of full-size simulation after TCV.
- Validation on COMPASS will include electron temperature and plasma potential fluctuations.

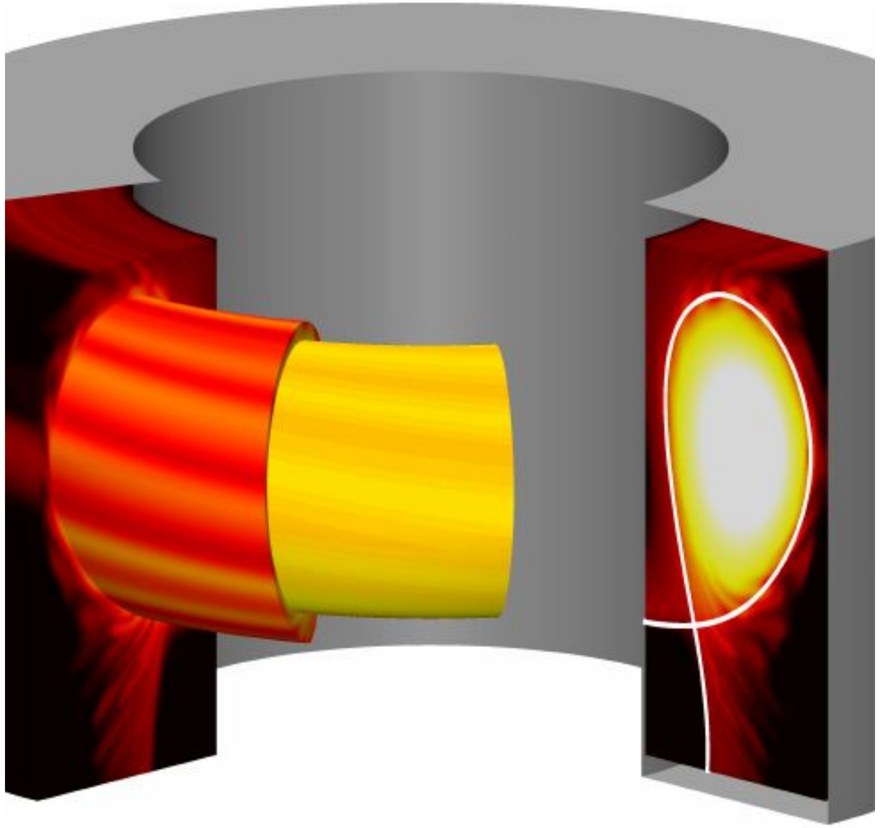

EQUATIONS

- Braginskii equations are solved, Boussinesq approximation is not used.
- 7 fields are evolved during each step:
  - Density, electron and ion parallel velocity, vorticity, electron and ion temperature, and psi (if electromagnetic effects are enabled).
- If kinetic neutrals are included:
  - Neutral density, and neutral parallel velocity.

$$\nabla\cdot\left(n\nabla_\perp\phi\right)=\Omega-\frac{\nabla_\perp^2 p_i}{e},$$

$$\left(\nabla_\perp^2-\frac{e^2\mu_0}{m_e}n\right)v_{\parallel e}=\nabla_\perp^2 U_{\parallel e}-\frac{e^2\mu_0}{m_e}nv_{\parallel i}+\frac{e^2\mu_0}{m_e}\bar{j}_\parallel .$$

$$U_{\parallel e}=v_{\parallel e}+e\psi/m_e$$

Particle confinement

$$\frac{\partial n}{\partial t}=-\frac{1}{B}[\phi,n]+\frac{2}{eB}\Big[C(p_e)-nC(\phi)\Big]-\nabla_\parallel(nv_{\parallel e})+D_n\nabla_\perp^2 n+s_n+\nu_{\rm iz}n_{\rm n}-\nu_{\rm rec}n\,, \quad (1)$$

Vorticity

$$\frac{\partial\Omega}{\partial t}=-\frac{1}{B}\nabla\cdot[\phi,\omega]-\nabla\cdot\left(v_{\parallel i}\nabla_\parallel\omega\right)+\frac{B\Omega_{ci}}{e}\nabla_\parallel j_\parallel+\frac{2\Omega_{ci}}{e}C(p_e+p_i)$$
$$+\frac{\Omega_{ci}}{3e}C(G_i)+D_\Omega\nabla_\perp^2\Omega-\frac{n_{\rm n}}{n}\nu_{\rm cx}\Omega\,, \quad (2)$$

Electron inertia

$$\frac{\partial U_{\parallel e}}{\partial t}=-\frac{1}{B}[\phi,v_{\parallel e}]-v_{\parallel e}\nabla_\parallel v_{\parallel e}+\frac{e}{m_e}\left(\frac{j_\parallel}{\sigma_\parallel}+\nabla_\parallel\phi-\frac{1}{en}\nabla_\parallel p_e-\frac{0.71}{e}\nabla_\parallel T_e-\frac{2}{3en}\nabla_\parallel G_e\right)$$
$$+D_{v_{\parallel e}}\nabla_\perp^2 v_{\parallel e}+\frac{n_{\rm n}}{n}(\nu_{\rm en}+2\nu_{\rm iz})(v_{\parallel n}-v_{\parallel e})\,, \quad (3)$$

ion inertia

$$\frac{\partial v_{\parallel i}}{\partial t}=-\frac{1}{B}[\phi,v_{\parallel i}]-v_{\parallel i}\nabla_\parallel v_{\parallel i}-\frac{1}{m_i n}\nabla_\parallel(p_e+p_i)-\frac{2}{3m_i n}\nabla_\parallel G_i$$
$$+D_{v_{\parallel i}}\nabla_\perp^2 v_{\parallel i}+\frac{n_{\rm n}}{n}(\nu_{\rm iz}+\nu_{\rm cx})(v_{\parallel n}-v_{\parallel i})\,, \quad (4)$$

electron energy confinement

$$\frac{\partial T_e}{\partial t}=-\frac{1}{B}[\phi,T_e]-v_{\parallel e}\nabla_\parallel T_e+\frac{2}{3}T_e\left[0.71\frac{\nabla_\parallel j_\parallel}{en}-\nabla_\parallel v_{\parallel e}\right]+\frac{4}{3}\frac{T_e}{eB}\left[\frac{7}{2}C(T_e)+\frac{T_e}{n}C(n)-eC(\phi)\right]$$
$$+\nabla_\parallel(\chi_{\parallel e}\nabla_\parallel T_e)+D_{T_e}\nabla_\perp^2 T_e+s_{T_e}-\frac{n_{\rm n}}{n}\nu_{\rm en}m_e\frac{2}{3}v_{\parallel e}(v_{\parallel n}-v_{\parallel e})$$
$$-2\frac{m_e}{m_i}\frac{1}{\tau_e}(T_e-T_i)+\frac{n_{\rm n}}{n}\nu_{\rm iz}\left[-\frac{2}{3}E_{\rm iz}-T_e+m_e v_{\parallel e}\left(v_{\parallel e}-\frac{4}{3}v_{\parallel n}\right)\right], \quad (5)$$

ion energy confinement

$$\frac{\partial T_i}{\partial t}=-\frac{1}{B}[\phi,T_i]-v_{\parallel i}\nabla_\parallel T_i+\frac{4}{3}\frac{T_i}{eB}\left[C(T_e)+\frac{T_e}{n}C(n)-eC(\phi)\right]-\frac{10}{3}\frac{T_i}{eB}C(T_i)$$
$$+\frac{2}{3}T_i\left[(v_{\parallel i}-v_{\parallel e})\frac{\nabla_\parallel n}{n}-\nabla_\parallel v_{\parallel e}\right]+\nabla_\parallel(\chi_{\parallel i}\nabla_\parallel T_i)+D_{T_i}\nabla_\perp^2 T_i+s_{T_i}$$
$$+2\frac{m_e}{m_i}\frac{1}{\tau_e}(T_e-T_i)+\frac{n_{\rm n}}{n}(\nu_{\rm iz}+\nu_{\rm cx})\left[T_n-T_i+\frac{1}{3}(v_{\parallel n}-v_{\parallel i})^2\right], \quad (6)$$

BOUNDARY CONDITIONS

- BCs play an important role in the simulation.
- Applied at the magnetic presheath.
- There are specific sets of BCs for plasma potential and for other fields.
- Plasma potential uses multiple conditions:
  - **Man** - Dirichlet, Neumann – fixing all fields.
  - **pAT** – fixing potential to ΛT_e , other fields Man.
  - **Tar** - fixing potential to ΛT_e, others Mag
  - **Rob**in – allowing potential to vary from ΛT_e.
  - **Mag**netic – full conductive condition.

$$v_{\parallel i} = \pm c_s \sqrt{1 + \frac{T_i}{T_e}},$$
$$v_{\parallel e} = \pm c_s \sqrt{1 + \frac{T_i}{T_e}} \exp\left(\Lambda - \frac{e\phi}{T_e}\right),$$
$$\partial_s n = \mp \frac{n}{c_s \sqrt{1 + \frac{T_i}{T_e}}} \partial_s v_{\parallel i},$$
$$\partial_s T_e = \partial_s T_i = 0,$$
$$\Omega = \mp \frac{m_i n}{e} c_s \sqrt{1 + \frac{T_i}{T_e}} \partial^2_{ss} v_{\parallel i},$$
$$\partial_s \phi = \mp \frac{m_i c_s}{e \sqrt{1 + \frac{T_i}{T_e}}} \partial_s v_{\parallel i},$$

Man

$$\phi(x, z) = A$$

pAT

$$\phi(x, z) = \Lambda(x, z) T_e(x, z),$$
$$\Lambda(x, z) = \lambda - \sqrt{1 + \tau \frac{T_i(x, z)}{T_e(x, z)}}$$

Rob

$$\phi(x, z) = \Lambda(x, z) T_e(x, z) - R_{fac}(x) \partial_x \Psi(x) B_{sign}(x) T_e(x, z) \left(\partial_y n(x, z) + 1.71 \partial_y T_e(x, z)\right),$$

where

$$R_{fac}(x) = \sum_z \frac{T_e(x, z)}{c_s(x) \sqrt{1 + \tau \frac{T_i(x,z)}{T_e(x,z)}}} \mu \mu_{spitzer}(x) F_{fac},$$

Mag

$$\partial_y \phi(x, z) = -\frac{\frac{\partial_x \Psi}{|\partial_x \Psi|} c_s(x, z)}{\sqrt{1 + \tau \frac{T_i(x,z)}{T_e(x,z)}}} \partial_y v_{\parallel i}(x, z),$$

BOUNDARY CONDITIONS

- BCs play an important role in the simulation.
- Applied at the magnetic presheath.
- There are specific sets of BCs for plasma potential and for other fields.
- Plasma potential uses multiple conditions:
  - **Man** - Dirichlet, Neumann – fixing all fields.
  - **pAT** – fixing potential to ΛT_e , other fields Man.
  - **Tar** - fixing potential to ΛT_e, others Mag
  - **Rob**in – allowing potential to vary from ΛT_e.
  - **Mag**netic – full conductive condition.

$$v_{\parallel i} = \pm c_s \sqrt{1 + \frac{T_i}{T_e}},$$

$$v_{\parallel e} = \pm c_s \sqrt{1 + \frac{T_i}{T_e}} \exp\left(\Lambda - \frac{e\phi}{T_e}\right),$$

$$\partial_s n = \mp \frac{n}{c_s \sqrt{1 + \frac{T_i}{T_e}}} \partial_s v_{\parallel i},$$

$$\partial_s T_e = \partial_s T_i = 0,$$

$$\Omega = \mp \frac{m_i n}{e} c_s \sqrt{1 + \frac{T_i}{T_e}} \partial^2_{ss} v_{\parallel i},$$

$$\partial_s \phi = \mp \frac{m_i c_s}{e \sqrt{1 + \frac{T_i}{T_e}}} \partial_s v_{\parallel i},$$

Man

$$\phi(x, z) = A$$

pAT

$$\phi(x, z) = \Lambda(x, z) T_e(x, z),$$

$$\Lambda(x, z) = \lambda - \sqrt{1 + \tau \frac{T_i(x, z)}{T_e(x, z)}}$$

Rob

$$\phi(x, z) = \Lambda(x, z) T_e(x, z) - R_{fac}(x) \partial_x \Psi(x) B_{sign}(x) T_e(x, z) \left(\partial_y n(x, z) + 1.71 \partial_y T_e(x, z)\right),$$

where

$$R_{fac}(x) = \sum_z \frac{T_e(x, z)}{c_s(x) \sqrt{1 + \tau \frac{T_i(x,z)}{T_e(x,z)}}} \mu \mu_{spitzer}(x) F_{fac},$$

Mag

$$\partial_y \phi(x, z) = - \frac{\frac{\partial_x \Psi}{|\partial_x \Psi|} c_s(x, z)}{\sqrt{1 + \tau \frac{T_i(x,z)}{T_e(x,z)}}} \partial_y v_{\parallel i}(x, z),$$

BOUNDARY CONDITIONS

- BCs play an important role in the simulation.
- Applied at the magnetic presheath.
- There are specific sets of BCs for plasma potential and for other fields.
- Plasma potential uses multiple conditions:
  - **Man** - Dirichlet, Neumann – fixing all fields.
  - **pAT** – fixing potential to ΛT_e , other fields Man.
  - **Tar** - fixing potential to ΛT_e, others Mag
  - **Rob**in – allowing potential to vary from ΛT_e.
  - **Mag**netic – full conductive condition.

$$v_{\|i} = \pm c_s \sqrt{1 + \frac{T_i}{T_e}},$$
$$v_{\|e} = \pm c_s \sqrt{1 + \frac{T_i}{T_e}} \exp\left(\Lambda - \frac{e\phi}{T_e}\right),$$
$$\partial_s n = \mp \frac{n}{c_s \sqrt{1 + \frac{T_i}{T_e}}} \partial_s v_{\|i},$$
$$\partial_s T_e = \partial_s T_i = 0,$$
$$\Omega = \mp \frac{m_i n}{e} c_s \sqrt{1 + \frac{T_i}{T_e}} \partial_{ss}^2 v_{\|i},$$
$$\partial_s \phi = \mp \frac{m_i c_s}{e \sqrt{1 + \frac{T_i}{T_e}}} \partial_s v_{\|i},$$

Man

$$\phi(x,z) = A$$

pAT

$$\phi(x,z) = \Lambda(x,z) T_e(x,z),$$
$$\Lambda(x,z) = \lambda - \sqrt{1 + \tau \frac{T_i(x,z)}{T_e(x,z)}}$$

Rob

$$\phi(x,z) = \Lambda(x,z) T_e(x,z) - R_{fac}(x) \partial_x \Psi(x) B_{sign}(x) T_e(x,z) \left(\partial_y n(x,z) + 1.71 \partial_y T_e(x,z)\right),$$

where

$$R_{fac}(x) = \sum_z \frac{T_e(x,z)}{c_s(x) \sqrt{1 + \tau \frac{T_i(x,z)}{T_e(x,z)}}} \mu \mu_{spitzer}(x) F_{fac},$$

Mag

$$\partial_y \phi(x,z) = -\frac{\frac{\partial_x \Psi}{|\partial_x \Psi|} c_s(x,z)}{\sqrt{1 + \tau \frac{T_i(x,z)}{T_e(x,z)}}} \partial_y v_{\|i}(x,z),$$

BOUNDARY CONDITIONS

- BCs play an important role in the simulation.
- Applied at the magnetic presheath.
- There are specific sets of BCs for plasma potential and for other fields.
- Plasma potential uses multiple conditions:
  - **Man** - Dirichlet, Neumann – fixing all fields.
  - **pAT** – fixing potential to ΛT_e , other fields Man.
  - **Tar** - fixing potential to ΛT_e, others Mag.
  - **Rob**in – allowing potential to vary from ΛT_e.
  - **Mag**netic – full conductive condition.

$$v_{\parallel i} = \pm c_s \sqrt{1 + \frac{T_i}{T_e}},$$

$$v_{\parallel e} = \pm c_s \sqrt{1 + \frac{T_i}{T_e}} \exp\left(\Lambda - \frac{e\phi}{T_e}\right)$$

$$\partial_s n = \mp \frac{n}{c_s \sqrt{1 + \frac{T_i}{T_e}}} \partial_s v_{\parallel i},$$

$$\partial_s T_e = \partial_s T_i = 0,$$

$$\Omega = \mp \frac{m_i n}{e} c_s \sqrt{1 + \frac{T_i}{T_e}} \partial^2_{ss} v_{\parallel i},$$

$$\partial_s \phi = \mp \frac{m_i c_s}{e \sqrt{1 + \frac{T_i}{T_e}}} \partial_s v_{\parallel i},$$

Man

$$\phi(x, z) = A$$

pAT

$$\phi(x, z) = \Lambda(x, z) T_e(x, z),$$

$$\Lambda(x, z) = \lambda - \sqrt{1 + \tau \frac{T_i(x, z)}{T_e(x, z)}}$$

Rob

$$\phi(x, z) = \Lambda(x, z) T_e(x, z) - R_{fac}(x) \partial_x \Psi(x) B_{sign}(x) T_e(x, z) \left(\partial_y n(x, z) + 1.71 \partial_y T_e(x, z)\right),$$

where

$$R_{fac}(x) = \sum_z \frac{T_e(x, z)}{c_s(x) \sqrt{1 + \tau \frac{T_i(x, z)}{T_e(x, z)}}} \mu \mu_{spitzer}(x) F_{fac},$$

Mag

$$\partial_y \phi(x, z) = - \frac{\frac{\partial_x \Psi}{|\partial_x \Psi|} c_s(x, z)}{\sqrt{1 + \tau \frac{T_i(x, z)}{T_e(x, z)}}} \partial_y v_{\parallel i}(x, z),$$

BOUNDARY CONDITIONS

- BCs play an important role in the simulation.
- Applied at the magnetic presheath.
- There are specific sets of BCs for plasma potential and for other fields.
- Plasma potential uses multiple conditions:
  - **Man** - Dirichlet, Neumann – fixing all fields.
  - **pAT** – fixing potential to ΛT_e , other fields Man.
  - **Tar** - fixing potential to ΛT_e, others Mag
  - **Rob**in – allowing potential to vary from ΛT_e.
  - **Mag**netic – full conductive condition.

Man

$$\phi(x,z) = A$$

pAT

$$\phi(x,z) = \Lambda(x,z)T_e(x,z),$$

$$\Lambda(x,z) = \lambda - \sqrt{1+\tau\frac{T_i(x,z)}{T_e(x,z)}}$$

$$v_{\|i} = \pm c_s\sqrt{1+\frac{T_i}{T_e}},$$

$$v_{\|e} = \pm c_s\sqrt{1+\frac{T_i}{T_e}}\exp\left(\Lambda - \frac{e\phi}{T_e}\right),$$

$$\partial_s n = \mp\frac{n}{c_s\sqrt{1+\frac{T_i}{T_e}}}\partial_s v_{\|i},$$

$$\partial_s T_e = \partial_s T_i = 0,$$

$$\Omega = \mp\frac{m_i n}{e}c_s\sqrt{1+\frac{T_i}{T_e}}\partial^2_{ss}v_{\|i},$$

$$\partial_s\phi = \mp\frac{m_i c_s}{e\sqrt{1+\frac{T_i}{T_e}}}\partial_s v_{\|i},$$

Rob

$$\phi(x,z) = \Lambda(x,z)T_e(x,z) - R_{fac}(x)\partial_x\Psi(x)B_{sign}(x)T_e(x,z)\left(\partial_y n(x,z) + 1.71\partial_y T_e(x,z)\right),$$

where

$$R_{fac}(x) = \sum_z \frac{T_e(x,z)}{c_s(x)\sqrt{1+\tau\frac{T_i(x,z)}{T_e(x,z)}}}\mu\mu_{spitzer}(x)F_{fac},$$

Mag

$$\partial_y\phi(x,z) = -\frac{\frac{\partial_x\Psi}{|\partial_x\Psi|}c_s(x,z)}{\sqrt{1+\tau\frac{T_i(x,z)}{T_e(x,z)}}}\partial_y v_{\|i}(x,z),$$

BOUNDARY CONDITIONS

- BCs play an important role in the simulation.
- Applied at the magnetic presheath.
- There are specific sets of BCs for plasma potential and for other fields.
- Plasma potential uses multiple conditions:
  - **Man** - Dirichlet, Neumann – fixing all fields.
  - **pAT** – fixing potential to ΛT_e , other fields Man.
  - **Tar** - fixing potential to ΛT_e, others Mag
  - **Robin** – allowing potential to vary from ΛT_e.
  - **Mag**netic – full conductive condition.

$$v_{\|i} = \pm c_s \sqrt{1+\frac{T_i}{T_e}},$$
$$v_{\|e} = \pm c_s \sqrt{1+\frac{T_i}{T_e}} \exp\left(\Lambda - \frac{e\phi}{T_e}\right),$$
$$\partial_s n = \mp \frac{n}{c_s\sqrt{1+\frac{T_i}{T_e}}} \partial_s v_{\|i},$$
$$\partial_s T_e = \partial_s T_i = 0,$$
$$\Omega = \mp \frac{m_i n}{e} c_s \sqrt{1+\frac{T_i}{T_e}} \partial^2_{ss} v_{\|i},$$
$$\partial_s \phi = \mp \frac{m_i c_s}{e\sqrt{1+\frac{T_i}{T_e}}} \partial_s v_{\|i},$$

Man

$$\phi(x,z) = A$$

pAT

$$\phi(x,z) = \Lambda(x,z) T_e(x,z),$$
$$\Lambda(x,z) = \lambda - \sqrt{1+\tau \frac{T_i(x,z)}{T_e(x,z)}}$$

Rob

$$\phi(x,z) = \Lambda(x,z) T_e(x,z) - R_{fac}(x) \partial_x \Psi(x) B_{sign}(x) T_e(x,z) \left(\partial_y n(x,z) + 1.71 \partial_y T_e(x,z)\right),$$

where

$$R_{fac}(x) = \sum_z \frac{T_e(x,z)}{c_s(x)\sqrt{1+\tau\frac{T_i(x,z)}{T_e(x,z)}}} \mu \mu_{spitzer}(x) F_{fac},$$

Mag

$$\partial_y \phi(x,z) = -\frac{\frac{\partial_x \Psi}{|\partial_x \Psi|} c_s(x,z)}{\sqrt{1+\tau\frac{T_i(x,z)}{T_e(x,z)}}} \partial_y v_{\|i}(x,z),$$

ROBIN BOUNDARY CONDITION

$$v_{\|i} = \pm c_s \sqrt{1 + \frac{T_i}{T_e}},$$

$$v_{\|e} = \pm c_s \sqrt{1 + \frac{T_i}{T_e}} \exp\left(\Lambda - \frac{e\phi}{T_e}\right),$$

BOUNDARY CONDITIONS

$$\phi(x,z) = \Lambda(x,z)T_\mathrm{e}(x,z) - R_\mathrm{fac}(x)\partial_x\Psi(x)B_\mathrm{sign}(x)T_\mathrm{e}(x,z)\left(\partial_y n(x,z) + 1.71\partial_y T_\mathrm{e}(x,z)\right),$$

where

$$R_\mathrm{fac}(x) = \sum_z \frac{T_\mathrm{e}(x,z)}{c_\mathrm{s}(x)\sqrt{1+\tau\frac{T_\mathrm{i}(x,z)}{T_\mathrm{e}(x,z)}}}\mu\mu_\mathrm{spitzer}(x)F_\mathrm{fac},$$

- **Tar** - fixing potential to ΛT_e, others Mag
- **Rob**in – allowing potential to vary from ΛT_e.
- **Mag**netic – full conductive condition.

Mag

$$\partial_y\phi(x,z) = -\frac{\frac{\partial_x\Psi}{|\partial_x\Psi|}c_\mathrm{s}(x,z)}{\sqrt{1+\tau\frac{T_\mathrm{i}(x,z)}{T_\mathrm{e}(x,z)}}}\partial_y v_{\|\mathrm{i}}(x,z),$$

COMPASS SET OF BCS

- In the case of COMPASS simulation, all the **Tar**, **Rob**, and **Mag**netic BC were applied on the bottom boundary - the divertor position.
- **Tar** condition (potential fixed to λT_e) used at left and top boundary.
- **Dirichlet** and **Neumann** conditions are set on right boundary for all fields.
- It was shown, turbulent structures disappear before touching the right boundary.
- Influence of the Dirichlet boundary is therefore not propagating inside plasma.

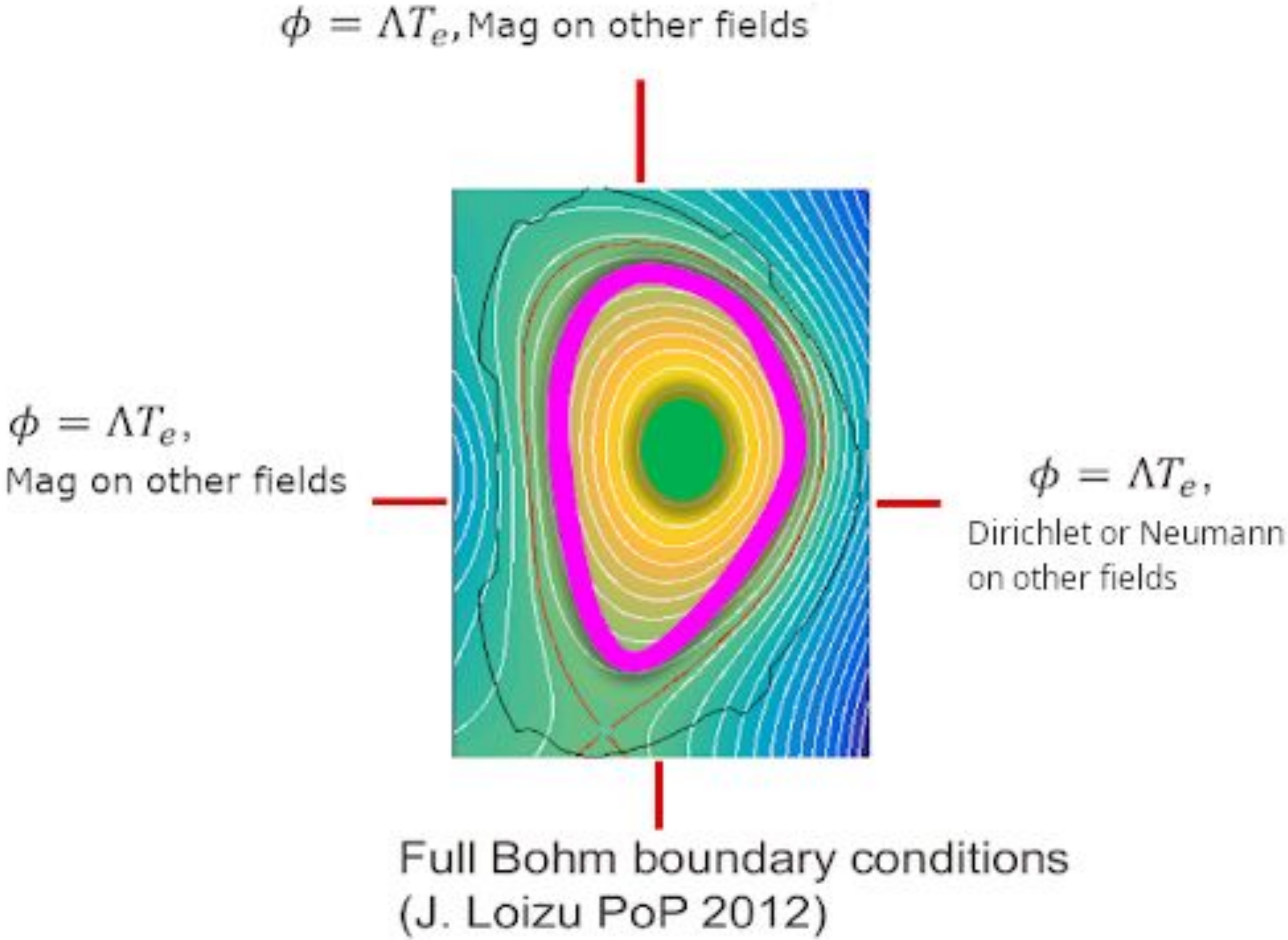

AN IMPACT OF BCs ON TURBULENCE

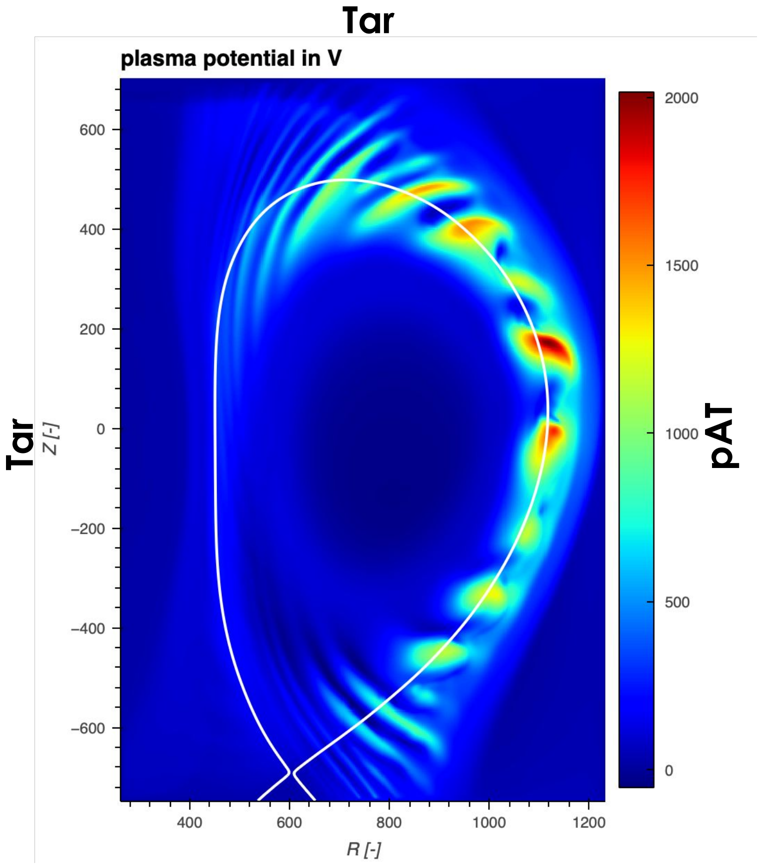

Tar
Potential fixed to ΛT_e,
Other fields Mag

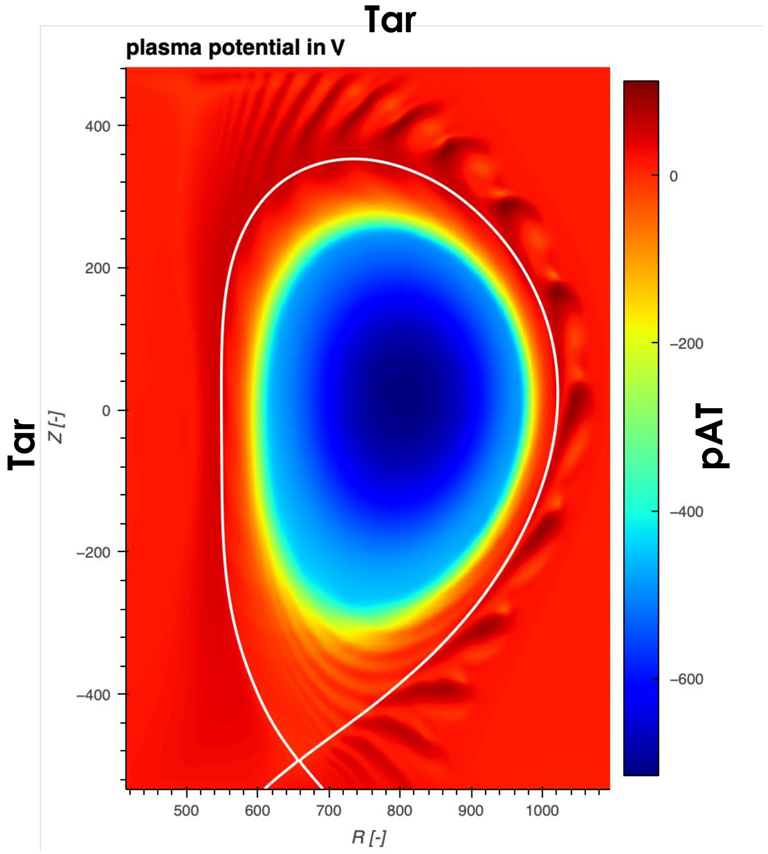

Rob
Potential can vary ΛT_e,
Other fields Mag

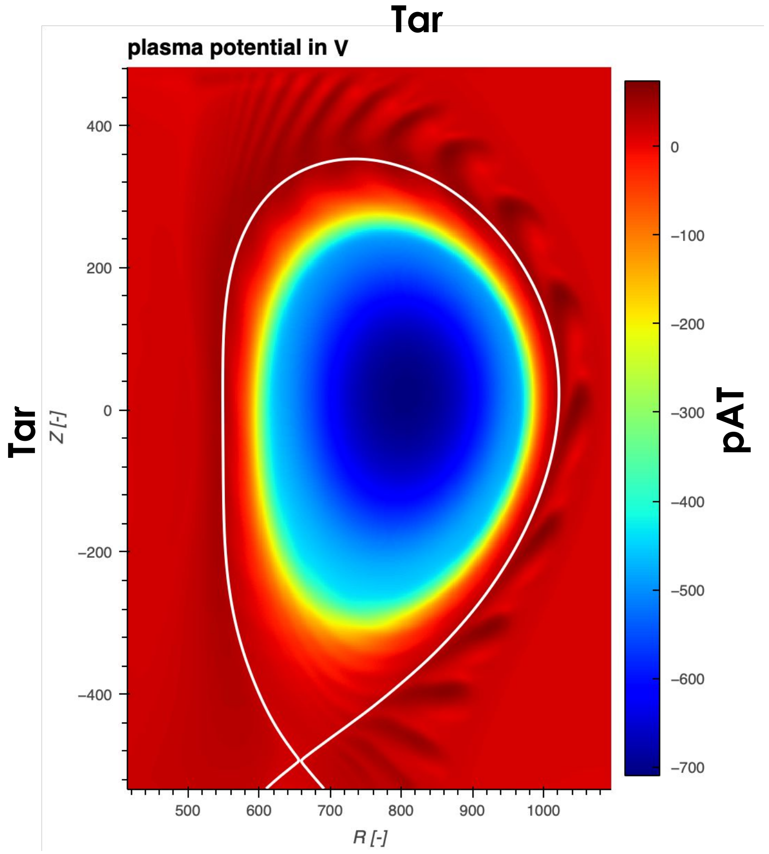

Mag
Full conductive

ROBIN VS MAG BC

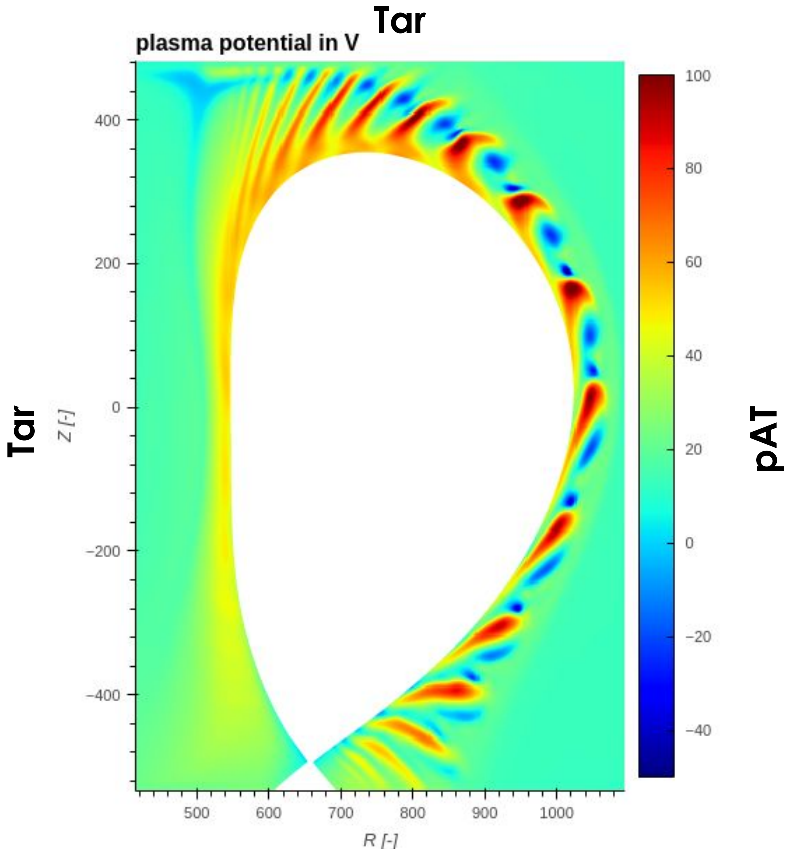

Rob
Potential can vary ΛT_e,
Other fields Mag

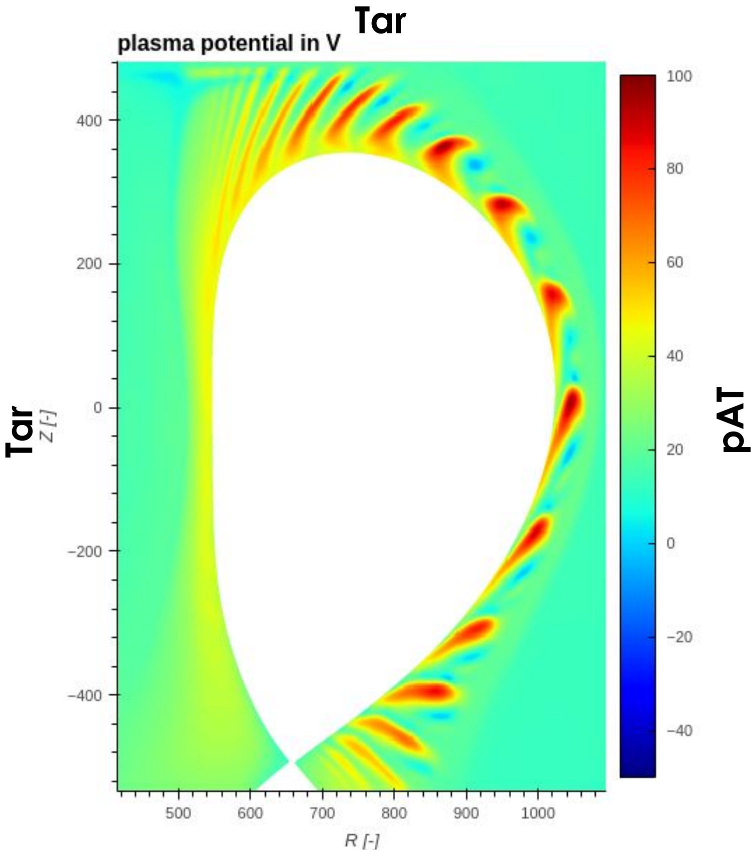

Mag
Full conductive

- Similar blob shapes and amplitudes are observed for both the **Rob** and **Mag**.
- A bit lower amplitudes of negative structures for the **Rob** BC.
- Both **Rob** and **Mag** should be equivalent to each other.
- Usage of **Mag** is however prefered, **Rob** used for transition from **Tar**.
- Furthermore, problem with Poisson solver and **Rob** BC in COMPASS simulation leading to code slowening.

ELECTRON PARALLEL VELOCITIES IN MAG

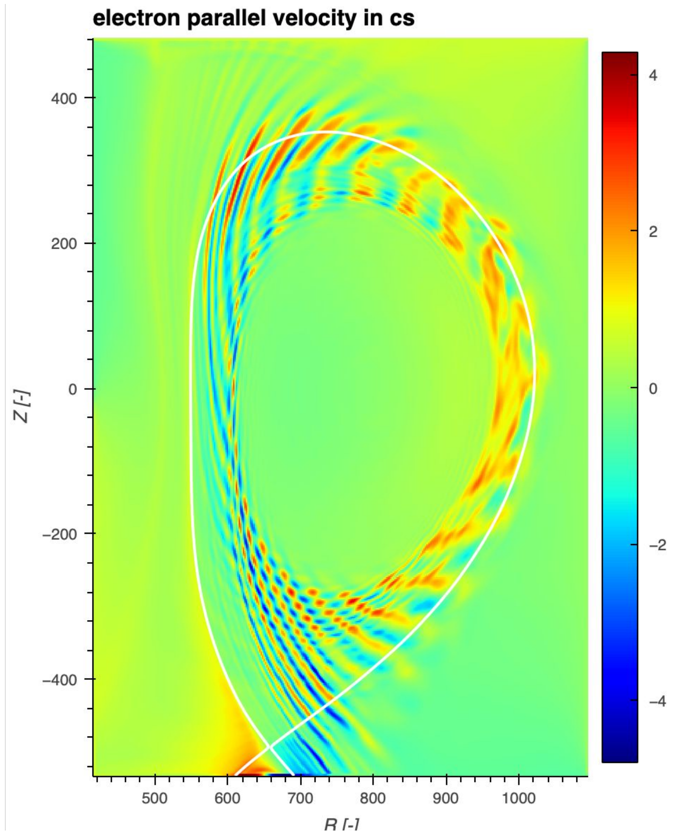

Electron parallel velocity

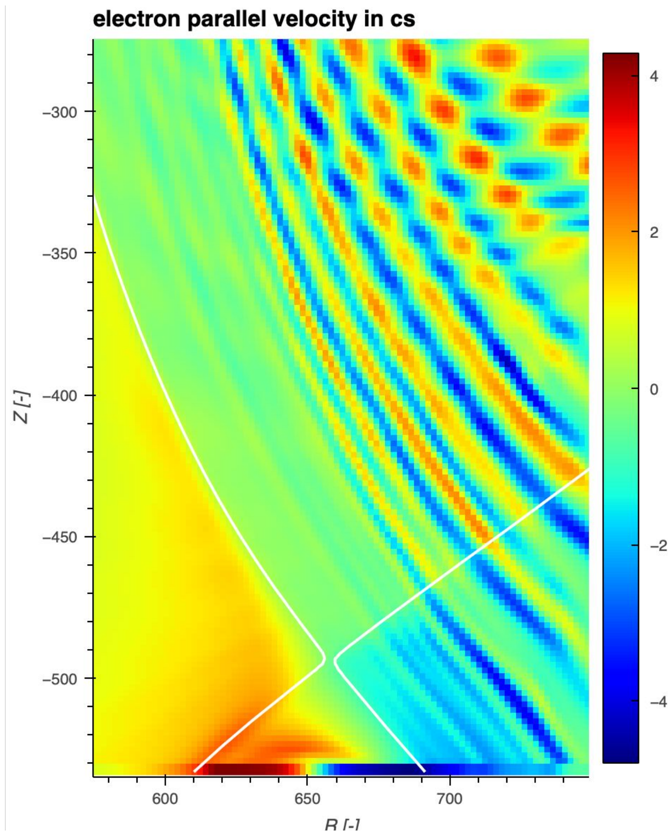

Electron parallel velocity
Zoomed on FPR

- Significantly higher values (~3x)of vpare for **Mag** BC.
- Sign represents direction with respect to magnetic field lines alignment.
- The 1D profile is smoothed by Tanh function in ghost cells where mag. Field is tangent to surface.
- Electron and ion parallel velocity set to 0 between the two regions (plus zero derivative of vpari).

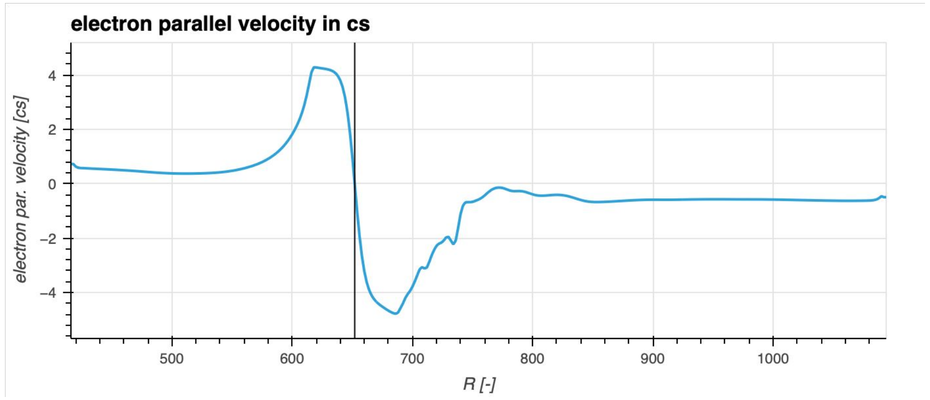

1D profile of electron parallel velocity at the bottom boundary

VERTICAL ELECTRIC FIELD AT BC

1)

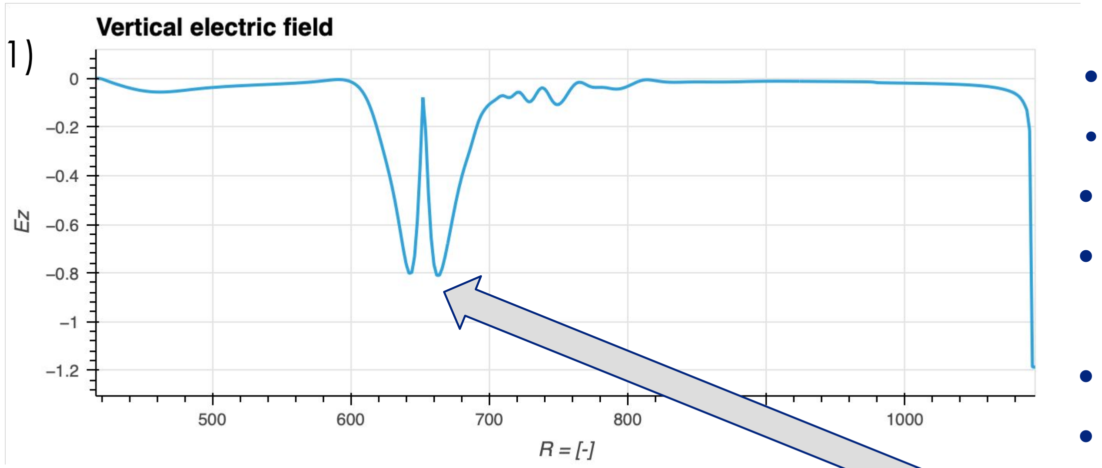

- **Ez calculated between ghost cells!**
- Crash of vertical electric field at inner strike point.
- Hard limit in code cutting Ez > 0 to 0
- The point in middle forced to zero by setting derivative of ion parallel velocity to zero.
- Causing parallel electron velocity to increase.
- Leading to crash in consequence.
- Self-refresh after several time units.

$$v_{\parallel i} = \pm c_s \sqrt{1 + \frac{T_i}{T_e}},$$

$$v_{\parallel e} = \pm c_s \sqrt{1 + \frac{T_i}{T_e}} \exp\left(\Lambda - \frac{e\phi}{T_e}\right),$$

$$\partial_s n = \mp \frac{n}{c_s \sqrt{1 + \frac{T_i}{T_e}}} \partial_s v_{\parallel i},$$

$$\partial_s T_e = \partial_s T_i = 0,$$

$$\Omega = \mp \frac{m_i n}{e} c_s \sqrt{1 + \frac{T_i}{T_e}} \partial_{ss}^2 v_{\parallel i},$$

$$\partial_s \phi = \mp \frac{m_i c_s}{e \sqrt{1 + \frac{T_i}{T_e}}} \partial_s v_{\parallel i},$$

Initial Ez

3)

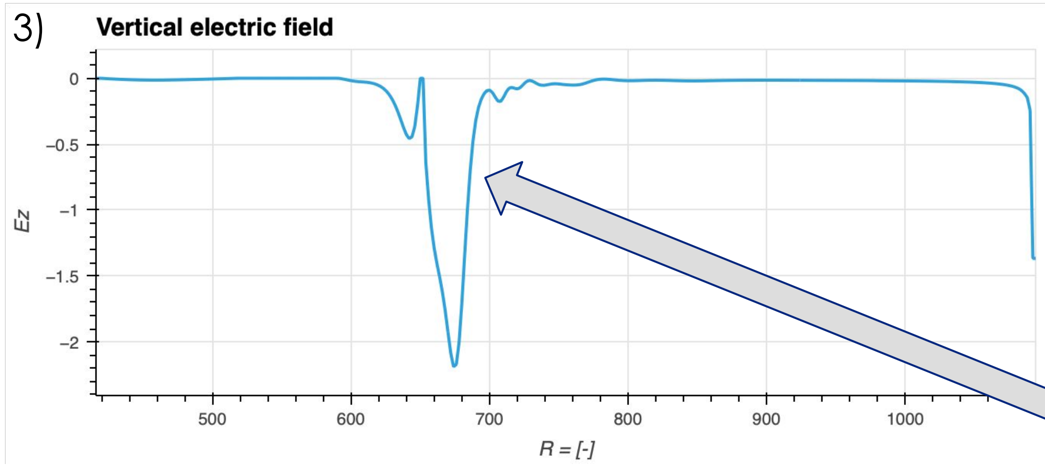

Ez self-refreshed

2)

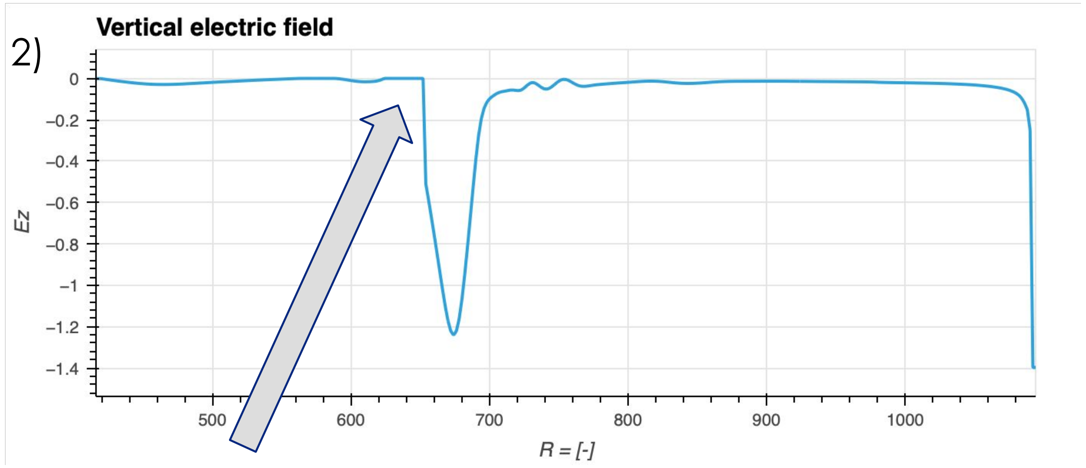

Ez crash

BOUNDARY PLOTS

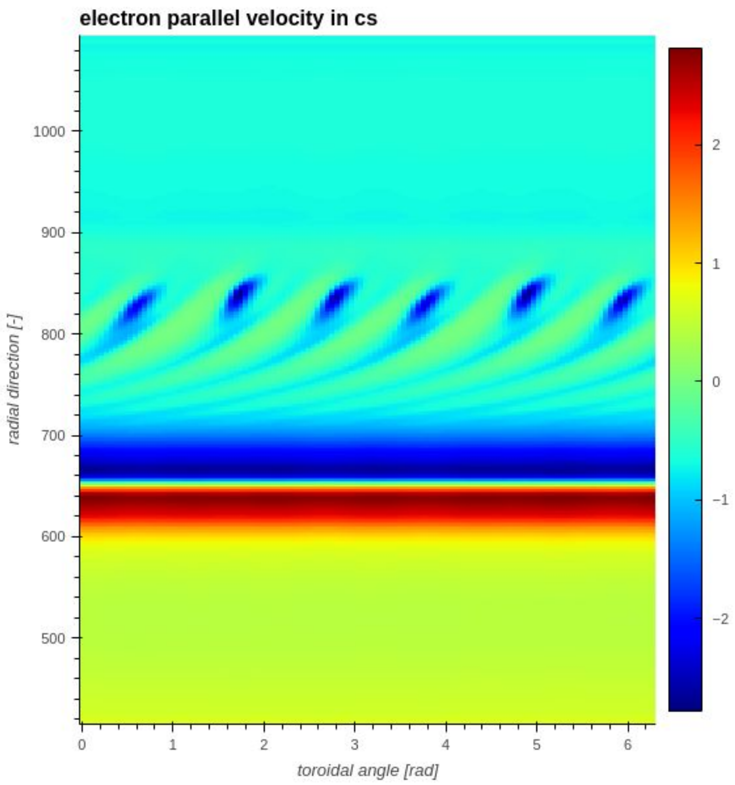

Normal values

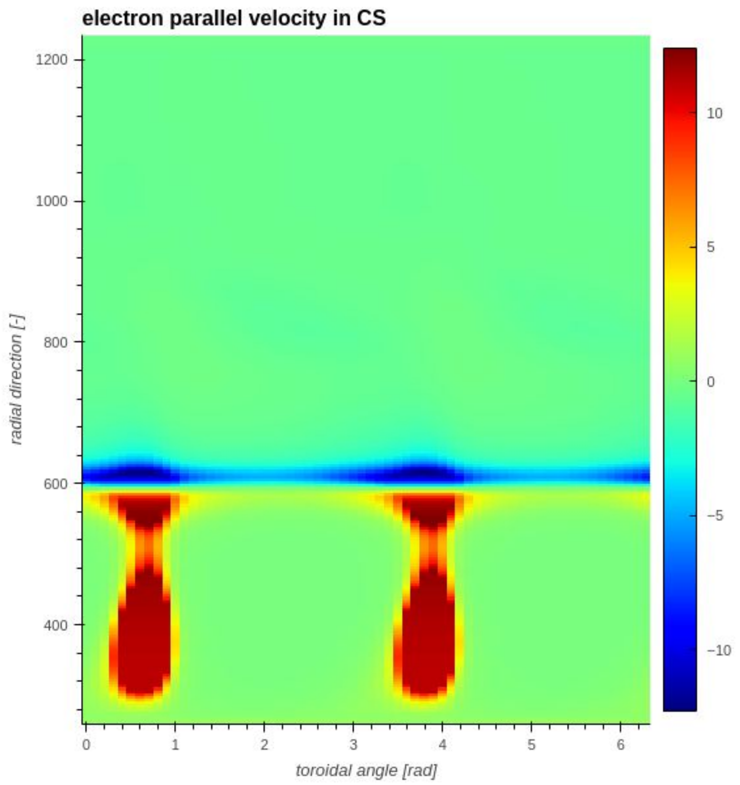

Crash in electron velocity

- The crash in electron parallel velocities, caused by vertical electric field, was threatened by adjusting the mass ratio and the sheath drop $\mathbf{\Lambda}$.
- The mechanism of positive vertical electric field formation is however still not well understood.
- Already appeared several times using **Mag** BC in past.
- Since now, the problem did not appear again.

SUMMARY

- COMPASS simulation showed significant impact of BCs on simulation:
  - **Tar** condition caused huge amplitudes in potential, exceeding 2 000 V leading to crash.
  - Both **Rob**in and **Mag**netic BCs showed similar turbulence properties.
- Problems with Poisson solver combined with **Robin** boundary condition were observed.
- **Mag**netic boundary condition performed best, however, problems with vertical electric field were observed:
  - Increasing Ez caused acceleration of electrons and simulation crash.
  - The problem however fixed itself after enough simulation time and mass ratio adjustment.
  - This mechanism must be further investigated.
  - Since now, the problem with the bottom boundary did not happen again.

REFERENCES

1. M. Giacomin et al J. Comput. Phys. 463 (2022) 111294 (The GBS code for the self-consistent simulation of plasma turbulence and kinetic neutral dynamics in the tokamak boundary)
2. M. Giacomin *et al* 2021 *Nucl. Fusion* **61** 076002 (Theory-based scaling laws of near and far scrape-off layer widths in single-null L-mode discharges)

EUROPEAN UNION
European Structural and Investment Funds
Operational Programme Research,
Development and Education

MINISTRY OF EDUCATION,
YOUTH AND SPORTS